Biochimica et Biophysica Acta 1848 (2015) 869–877

Contents lists available at ScienceDirect

Biochimica et Biophysica Acta

journal homepage: www.elsevier.com/locate/bbamem

The uptake of HIV Tat peptide proceeds via two pathways which differ from macropinocytosis

Nadav Ben-Dov [1], Rafi Korenstein *

Department of Physiology and Pharmacology, Faculty of Medicine, Tel-Aviv University, 69978 Tel-Aviv, Israel

ARTICLE INFO

Article history:
Received 15 August 2014
Received in revised form 16 November 2014
Accepted 16 December 2014
Available online 24 December 2014

Keywords:
Cell penetrating peptide
Tat peptide
Endocytosis
Plasma membrane
Membrane translocation

ABSTRACT

Cell penetrating peptides (CPPs) have been extensively studied as vectors for cellular delivery of therapeutic molecules, yet the identity of their uptake routes remained unclear and is still under debate. In this study we provide new insights into CPP entry routes by quantitatively measuring the intracellular uptake of FAM-labeled Tat-peptide under rigorous kinetic and thermal conditions. The uptake of Tat-peptide between 4 and 15 °C corresponds to $Q_{10} = 1.1$, proceeding through a prompt (<5 min), temperature-independent process, suggesting direct membrane translocation. At longer durations, Tat rate of uptake shows linear dependence on temperature with $Q_{10} = 1.44$, accompanied by activation energy $E_a = 4.45$ Kcal/mole. These values are significantly lower than those we found for the macropinocytosis probe dextran ($Q_{10} = 2.2$ and $E_a = 7.2$ Kcal/mole) which possesses an exponential dependence on temperature, characteristic of endocytosis processes. Tat-peptide and dextran do not interfere with each other's uptake rate and the ratio of Tat-peptide uptake to its extracellular concentration is ~15 times higher than that for dextran. In addition, Phloretin, a modulator of cell membrane dipole potential, is shown to increase dextran uptake but to reduce that of Tat. We conclude that the uptake of Tat differs from that of dextran in all parameters. Tat uptake proceeds by dual entry routes which differ by their energy dependence.

1. Introduction

Cell penetrating peptides (CPP) have been highly praised for their ability to transport impermeable cargo across the cells' plasma membrane. However, despite the vast research conducted to explore the mode of their action, the mechanism underlying this phenomenon is still debated and existing studies do not yield coherent mechanistic information. Reports are abundant but contradicting; some inhibitors of endocytosis pathways can partially affect CPP uptake while others do not, implying that CPP share certain fundamental mechanisms with endocytosis [1–5]. Few reports have studied the kinetics of CPP uptake [6] at 37 °C, 25 °C or 4 °C but none have challenged the temperature range in detail. The internalization of CPP at low temperature was confirmed or opposed by a large number of studies [7], most obtained from fluorescence confocal imaging. However, the accuracy of this qualitative image analysis is constrained by fixation and staining techniques and is limited by the signal/noise threshold [6].

Models of CPP translocation across plasma membranes apply to small amphipathic alpha-helix secondary structures, a feature shared by many CPPs. There is evidence that many of the most well studied peptides are able to deliver relatively small cargo directly across the plasma membrane, such as fluorescent probes and hydrophobic adducts (e.g. short peptide sequences). The evidence also supports the involvement of endocytic pathways in CPP uptake [8]. Direct translocation of large conjugates attached to the CPP through the cell membrane involves an extensive destabilization of the membrane, which is not compatible with the low cytotoxicity usually associated with the membrane translocation of CPPs and their conjugates [4]. Accordingly, alternative mechanisms should play a role in peptide internalization, especially when conjugated with high molecular weight cargo.

Endocytosis is commonly governed by cellular machinery, involving membrane curve forming proteins (e.g. BAR or epsin), vesicle coat proteins (e.g. caveolin and clathrin) and vesicle scission proteins (e.g. dynamin GTPase) [9]. However, endocytic vesicles are also formed when these proteins are inhibited or absent altogether, suggesting that other less defined mechanisms exist. Several clathrin/caveolin independent endocytic pathways have been found, such as flotillin coated vesicles, GPI-AP enriched compartments (GEEC) and other pathways which are characterized by their dependence on small G proteins, i.e. RhoA, CDC42 or ARF6 [10,11] or by their membrane folding mechanism, such as proton-induced endocytosis [12,13]. It has been convincingly shown that CPP uptake is unlikely to be associated with clathrin and caveolin dependent endocytosis by inducing specific mutations in the clathrin, dynamin or caveolin proteins [14,15] and by siRNA methods that inhibit endocytic pathways regulated by clathrin heavy chain,

* Corresponding author at: Dept. of Physiology and Pharmacology, Faculty of Medicine, Tel-Aviv University, Israel. Tel.: +972 3 6406042; fax: +972 3 6408982.
E-mail addresses: nadavbe4@tx.technion.ac.il (N. Ben-Dov), korens@post.tau.ac.il (R. Korenstein).
[1] Present address: Dept. of Biotechnology and Food Engineering, Technion, Institute of Technology, Haifa, Israel.

http://dx.doi.org/10.1016/j.bbamem.2014.12.015
0005-2736/

flotillin-1, caveolin-1, dynamin-2 and Pak-1, which were unable to significantly inhibit CPP uptake [16]. Macropinocytosis (MPC) has been regarded as the pathway for CPP endocytosis, based on the findings that some inhibitors of fluid-phase uptake can partially inhibit CPP uptake. These inhibitors are not highly specific to MPC but are rather modifiers of the actin cytoskeleton organization, an element crucial for executing force actuation on the plasma membrane leading to membrane projection or ruffling. The finding that a certain inhibitor attenuates the internalization of different cargos implies that the uptake of these cargos shares a common denominator but does not necessarily undergo a similar mechanism of uptake. One must therefore consider that the dependence of CPP endocytosis on actin organization [16] may stem from the role of actin in vesicle constriction and scission rather than from membrane ruffling.

For studying the correlations between MPC pathway and CPP uptake, we chose to employ methods that alter the physical properties of the plasma membrane but do not impose detectable changes in cytoskeletal organization. We have analyzed the uptake rate of HIV-Tat peptide and compared it to the uptake of a fluid-phase probe dextran, known to progress through MPC. The uptake of these two well-known probes was studied as a function of temperature and membrane modifying agents. The relative contribution of direct Tat translocation across the cell membrane and the role played by the membrane's fluidity and the intra-membrane dipole potential on CPP uptake were studied by enriching the cell membrane with cholesterol, 6-ketocholestanol or phloretin.

2. Methods

2.1. Materials

Phosphate buffered saline (PBS), PBS free of Ca^{+2} and Mg^{+2}, Dulbecco's Modified Eagle Medium, 4.5 mg/ml glucose (DMEM), fetal calf serum (FCS), trypsin solution (0.25% with 0.05% EDTA), antibiotics solution of penicillin 10,000 unit/ml, streptomycin 10 mg/ml, nistatin 1250 unit/ml (PSN) L-glutamine solution (200 mM), 4-(2-hydroxyethyl)-1-piperazineethanesulfonic acid, 1 M (HEPES) and Tryphan-blue 0.4% (TB) were purchased from Biological Industries, Beit Ha'emek, Israel. Dextran-FITC (38 kD), dextran-TRITC (10 kD), phaloidine-TRITC, cholesterol (as methyl-β-cylodextrin solution), 6-ketocholestanol (6KC), phloretin, nigericin, wortmannin, 1-(4-trimethylammoniophenyl)-6-diphenyl-1,3,5-hexatriene (TMA-DPH) and chemicals for modified Karnovsky's fixative solution (2× strength: 6% paraformaldehyde, 1% glutaraldehyde and 0.2% Triton X-100 in 0.2 M cacodylate buffer) were purchased from Sigma-Aldrich, Rehovot, Israel. Tat peptide (YGRKKRRQRRR)-FAM labeled, was purchased from AnaSpec, Fremont, CA USA).

2.2. Flow cytometry

Flow cytometry analysis was carried out employing FACScalibur (Becton@Dickson, San Jose, CA). 10,000 cells were measured per sample and data analysis was performed using cyflogic 1.2.1 application software (CyFlo LTD, Finland). Fluorescein and propidium iodide (PI) were excited at 488 nm and their fluorescence was detected using 530/30 nm and 580/30 nm filters, respectively. Rhodamine fluorescence was excited at 561 nm and detected by a 600 nm high pass filter. To eliminate signals due to cellular fragments, only those events with forward and side scatter comparable to untreated cells were analyzed. Cells labeled by PI were considered damaged and rejected from analysis. Quantum FITC calibration kit (Bangs Labs, USA) was used in the quantification of fluorescein intensity. Upon establishing a calibration plot, no further adjustments of the instrument settings have been done (e.g. PMT amplifier gains and laser voltage).

2.3. Quantification by MESF

The cellular fluorescence intensity of fluorescein, measured by flow-cytometry, was calibrated in terms of units of Molecules of Equivalent Soluble Fluorochrome (MESF) using Quantum FITC MESF beads (Bangs Labs, USA). A 5 point calibration curve, overlapping the cells' fluorescence dynamic range was established from which the number of fluorescein molecules per cell was determined by linear regression. Tat molecules are in a 1:1 ratio to fluorescein, as each Tat peptide is conjugated to one fluorochrome. The ratio of FITC to dextran molecules was calculated using data from the manufacturer's certificate of analysis (COA) of the specific lot number we purchased, yielding 3.2 FITC molecules per dextran molecule of 38,400 Da. This ratio was verified by comparing the fluorescence intensity of 5 μM dextran-FITC and 5 μM Tat-FAM using a fluorescence plate reader. Thus the number of dextran molecule was calculated by dividing its MESF by 3.2.

2.4. Endocytosis studies

Fibroblast-like monkey kidney cells (COS-7, ATCC No. CRL-1651) were cultured in DMEM, supplemented with 2 mM L-glutamine, 10% FCS and 0.2% PSN solution and were grown at 37 ° C, in a humid atmosphere of 5% CO_2. For endocytosis experiments, COS-7 cells are seeded in 48-wells plates and grown to near-confluence (~80%). Prior to the experiment, the wells are washed once with 0.2 ml PBS and further incubated for 30 min at the designated experimental temperature. Temperature equilibration in a multiwell plate is not trivial and one must be aware of the discrepancy between the temperature given outside the plate (such as in plate-readers, temperature baths etc.) and the actual temperature measured within the wells. For 4 °C, the plates were covered with crushed ice. Otherwise, the plates were placed in a temperature-controlled dry bath and the well's temperature was determined by direct measurement in 12 wells selected at random using thin-wire thermocouple (CHY 508BR, Taiwan), allowing for ±0.5 °C well-to-well deviation. Following temperature stabilization, the wells were emptied and refilled with 0.15 ml of temperature equilibrated solution of a fluorescent probe in phenol-red free DMEM, and further incubated for durations of 10, 20 or 30 min. The well's temperature was verified at the start and finish of each incubation period.

When pre-treatment of the cells was required, the wells were washed once with PBS and refilled with 0.15 ml solution of either 0.1 mM cholesterol (employing a saturated MβC solution), 0.1 mM 6KC or 0.1 mM phloretin in PBS. PBS by itself was used for control. The cells were incubated for 30 min at 37 °C, washed twice with PBS, and exposed to a fluorescent probe solution (in phenol-red free DMEM) at 26 ± 1 °C for a further 30 min.

2.5. Cell harvest and washings

At the end of each experiment, the cells were washed in three consecutive steps. In the first step the wells were washed twice with cold, Ca^{2+} deficient, PBS (0.2 ml/well) to remove free dye from the cells. Each well was then filled with 0.1 ml Ca^{2+} deficient PBS and 0.1 ml trypsin solution and incubated at RT for 10 min. The content of each well was collected by repeated pipetting and transferred into a separate tube containing cold (5 °C) 0.5 ml blocking solution (phenol-red free DMEM with 10% FCS and 20 mM HEPES) and further incubated for 15 min at 5 °C. For the final washing step, the cells were sedimented in a cooled centrifuge (5 °C) at 500 *g* for 5 min to discard the solution. Next the cells were re-suspended in 0.2 ml of cold (8 ± 1 °C) K^+PBS in the presence of 10 μM nigericin to neutralize endosomal low pH. Prior to flow cytometry, 10 μg/ml of PI was added to the cell suspensions.

To validate our washing procedure, cells were incubated with Tat-FAM or dextran-FITC at temperatures in the range of 4–29 °C and washed as described above. The cells were analyzed twice consecutively

by a flow cytometer, first in the absence and then in the presence of the fluorescein quencher trypan blue (TB, 4.2 mM), as detailed earlier [12] and cells' fluorescence intensity was calibrated to MESF. The amount of fluorescein quenched by TB at each temperature, shown in Table 1, is not significantly different then that found at 4 °C, ($P = 0.203$ by single-factor ANOVA test) representing the probe fraction adsorbed to the cell's membrane. Following the extensive washing procedure, the cell's fluorescence intensity in the absence or presence of TB was analyzed by a paired *t*-test (see Table 2) to assert that no significant fraction of unbound Tat-FAM remains adsorbed to the cell's membrane.

2.6. Cell membrane anisotropy

Anisotropy (r) of TMA-DPH fluorescence (λ_{Ex} 360 nm, λ_{Em} 430 nm), was determined using the expression $r = (I_V - GI_H)/(I_V + G2I_H)$ where I represents the fluorescence intensity, V and H represent the vertical and horizontal orientation of the emission analysis polarizers, and G accounts for the sensitivity of the instrument. The fluorescence measurements were carried in a plate reader (Molecular Devices M5[e], Sunnyvale, CA, USA) with automatic determination of G values. Prior to each spectral measurement, the well's temperature was directly determined using the thin-wire thermocouple. Cells were first incubated at 37 °C with PBS alone or in the presence of either 0.1 mM cholesterol (as a saturated MβC solution), 0.1 mM 6KC or 0.1 mM phloretin for time periods of 15, 30, 45 or 60 min. To avoid possible interference of DMSO in the final dilution, phloretin and 6KC stock solutions were prepared at 100 mM concentration. Though TMA-DPH is virtually colorless in the aquatic phase, the presence of residual amphipathic molecules in the solution will lead to a high non-specific background. To overcome this situation, the plate wells were drained and washed twice in PBS before the addition of 5 μM TMA-DPH in PBS at 25 °C. The fluorescence intensity was recorded starting 10 min after the addition of TMA-DPH until 30 min has passed [17]. We found that under this procedure, the cells retain stable fluorescence polarization for 30 min at 25 °C, and the duration of the cell's incubation with the amphypathic agents had no significant effect on their membrane TMA-DPH polarization [18].

2.7. Fluorescent microscopy

Cell cultures were grown on glass cover slips coated with 2% gelatin. The cells were exposed to 1 μM wortmannin for 15 min, followed by addition of equal volume of modified karnovsky solution for fixation. The cells were post-stained with phalloidine-TRITC and digital images were acquired by a fluorescent microscope (Axio-observer Z1, Zeiss, Germany). Annotation was made using Illustrator CS software (Abode, USA).

2.8. Statistics

Results were collected from at least 3 independent experiments and statistical analyses were performed using Microsoft Excel spreadsheets. Descriptive statistics methods used are *t*-test, paired *t*-test and single variance ANOVA.

Table 1
Dextran adsorption to the cell membrane.

Temp during uptake (°C)	Independent repetitions (*n*)	[a]Fluorescein molecules	
		Average	s.d.
4	5	9194	6066
22	4	7505	3694
24	3	11,275	4885
27	3	5302	2022
29	3	7186	2731

[a] Calculated using MESF molecular scale.

Table 2
Tat-FAM adsorbed to the cell membrane following wash procedure, in the absence or presence of Trypan blue.

	t-test values	[a]Fluorescein molecules (−TB)	[a]Fluorescein molecules (+TB)
Mean		123,437	116,248
Deviation		23,306	23,722
Repeat (*n*)	18		
Paired *t*-value	5.3		
P (two-tails)	5.9×10^{-05}		

[a] Calculated using MESF molecular scale.

3. Results

The ability to differentiate between uptake and adsorption, especially when using high throughput flow-cytometry depends on the effectiveness of removal by washing as well as the quenching of the remaining fluorescent cargo adsorbed to the cell surface. The effectiveness of the cell washing procedure (which includes passive washes, enzymatic digestion, fluid shearing force and competition with serum constituents), was analytically examined by quenching extracellular fluorescein with TB [19], confirming the removal of adsorbed Tat-FAM from the cell membrane ($P < 0.01$ by a paired *t*-test). The remaining Tat-related cell fluorescence is attributed to cargo internalized or deeply embedded in the membrane. The use of microscopic imaging was not applied here, as this method offers inferior sensitivity and lower statistical power compared to flow cytometry, especially when working with low concentrations of probes located adjacent to the membrane.

3.1. The efficiency of Tat uptake as function of external concentration is higher than that of dextran

The extent of uptake was studied in cells exposed to different concentrations of Tat-FAM (1, 2.5 or 5 μM) or dextran-FITC (5, 10 or 15 μM). 38kD dextran was selected based on published studies, as an accredited MPC marker, most commonly used in the 40–70 kD size range [15,16,20,21]. The experimental protocol included incubation of COS-7 cells for 30 min at 37 °C with either of these two fluorescent molecules. This was followed by wash and harvest procedures as described in the Methods section. The extent of uptake was determined by flow-cytometry, where the cellular fluorescent intensity was expressed by the number of internalized fluorescent molecules using calibrated MESF microspheres. Fig. 1 presents the calculated number of

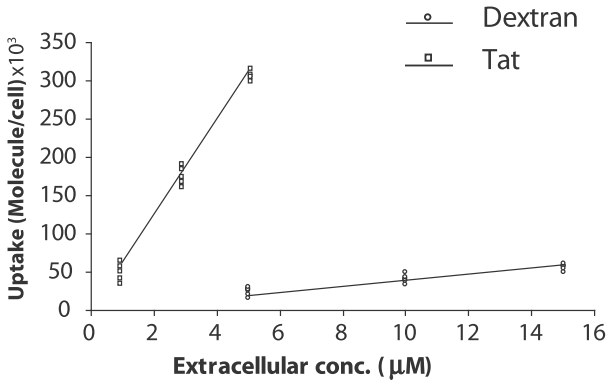

Fig. 1. Uptake of dextran and Tat-peptide as a function of their external concentrations. COS-7 cells were incubated in the presence of dextran-FITC or Tat-FAM at the indicated concentration for 30 min at 37 °C. Following wash and harvest procedures, cell analyses were conducted by flow-cytometry and cellular fluorescent intensity was calibrated using MESF microspheres. Least square regression, in terms of molecules/cell per μM, yields 62,692 ± 1770 (mean ± s.d.; $R^2 = 0.96$) for Tat uptake and 4,030 ± 104 (mean ± s.d.; $R^2 = 0.9$) for dextran. Each data point represents a triplicate average in one of five independent experiments.

internalized molecules per cell as a function of their extracellular concentration following 30 min of exposure. Least-square regression method of the experimental points yields a linear coefficient which represents the ratio of the intracellular number of molecules to the extracellular molar concentration. If we use a mean volume of 2361 μm^3 for a COS-7 cell [22], we can calculate the intracellular molar concentrations of Tat or dextran. The ratio of intracellular to extracellular concentration of the cargo probe is an expression of the uptake efficacy toward either Tat or dextran, following 30 min exposure to either of the probes at 37 °C. From Fig. 1, the cells' uptake per each μM external concentration (up to 15 μM) is 44 nM for Tat and 2.8 nM for dextran, which means that Tat uptake is ~15 times more efficient than that of dextran.

3.2. Tat and dextran do not interfere with each other's uptake

For the concurrent analysis of Tat and dextran uptake, we incubated the cells simultaneously with 2.5 μM Tat-FAM and 10 μM dextran-TRITC (10 kD). COS-7 cells were incubated with these two probes for 30 min at 37 °C and analyzed as detailed in the Methods section. Flow-cytometry was conducted using two separate laser lines (488 nm and 561 nm) to minimize interference, and the cells' geometric mean ± s.d. of the acquired fluorescence intensities are presented in Fig. 2. No significant difference was observed comparing the cellular fluorescent intensity of cells incubated with both fluorescent probes to those incubated with either Tat-FAM or dextran-TRITC alone ($P > 0.01$, two tail t-test, $n = 10$).

3.3. Tat and dextran uptake possesses different temperature profiles

Examining the dependence of the uptake of Tat-FAM (2.5 μM) or dextran-FITC (5 μM) on temperature was carried out by incubating the culture plates at different temperatures in the range of 4–37 °C for durations of 10, 20 or 30 min. Cell analyses were conducted by flow-cytometry and cellular fluorescence intensity was calibrated using MESF microspheres.

Fig. 3 presents the calculated number of internalized molecules as a function of incubation duration at the different temperatures. The datapoints obtained at each temperature are fitted by least-square linear regression and their linear coefficients and intercepts are presented in Fig. 4A, B and C. Notably, there is no significant difference in the rate of dextran and Tat uptake between 4 and 8 °C ($P > 0.05$) showing that the minimum uptake has taken place and therefore the 4 °C point was omitted from Fig. 4.

Fig. 4A and B reveals that the rate of Tat uptake as a function of temperature is linear while that of dextran has an exponential uptake

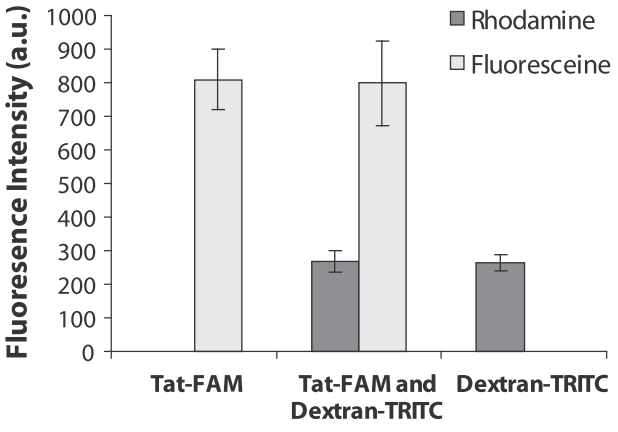

Fig. 2. Simultaneous uptake of Tat-peptide and dextran. COS-7 cells were simultaneously incubated in the presence of 10 μM dextran-TRITC and 2.5 μM Tat-FAM for 30 min at 37 °C. Following wash and harvest procedures, cell analyses were conducted by flow-cytometry using two laser lines (488 nm and 561 nm). Cell fluorescence intensity is presented as a geometric mean ± s.d. For each probe, the fluorescent intensity of the cells is similar to those incubated with both fluorescent probes ($P > 0.05$, two tail t-test, $n = 10$).

profile. The regression line intercept with the uptake ordinate axis, shown in Fig. 4C, reflects an initial interaction of Tat or dextran with the cell membrane that is temperature independent ($P > 0.05$ by one way ANOVA). From the data presented in Fig. 4C, it can be seen that dextran interaction is negligible but for Tat peptide, the extent of the initial interaction is high, yielding 25,000 ± 5000 Tat molecules/cell. It could be claimed that some of the fluorescence recorded during flow cytometry analysis is due to Tat adsorption to the membrane, especially at low temperatures. Therefore, the fraction of Tat-FAM adsorbed to the cell surface was challenged by the TB quenching test, as detailed in the Methods section and the efficiency of our cell washing procedure was confirmed.

The data presented in Fig. 4A and B is further interpreted using the Arrhenius equation:

$$\mathrm{Ln}(k) = \mathrm{Ln}(A) - Ea/R * 1/T \quad (1)$$

where k is the reaction rate, A is pre-exponential factor, E_a is the reaction activation energy, R is the gas constant and T is the temperature in °K.

This data transformation is presented in Fig. 4D, where Ln(k) is plotted as function of 1/T and the activation energy is calculated from the line slope (E_a/R). As the rate of uptake was found to reach its minimum at 8 °C (Fig. 3A, B), the 4 °C data point was excluded from Fig. 4D. The plot of dextran's uptake as function of temperature possesses a biphasic shape with a deflection point between 20 and 24 °C. The activation energy associated with dextran's rate of uptake, below and above the deflection point, is E_a ~ 4.7 Kcal/mole and E_a ~ 7.2 Kcal/mole, respectively. These results are in general agreement, albeit with lower E_a values, with previous reports of fluid phase endocytosis [23–25]. By contrast, the plot of Tat's uptake has a linear correlation with temperature possessing a monophasic activation energy of E_a ~ 4.45 Kcal/mole. The Q_{10} temperature coefficient was calculated from the data in Fig. 4A and B using the expression

$$Q_{10} = (R_2/R_1)^{10/(T_2-T_1)} \quad (2)$$

where R_i is the uptake rate found at temperature T_i. The Q_{10} between 20–29 °C and 27–37 °C are 1.8 and 1.4 for the uptake of Tat but 2.8 and 2.2 for the uptake of dextran.

3.4. Uptake is sensitive to the functionality of the actin cytoskeleton

In order to examine the involvement of actin-cytoskeleton in the uptake process we employed wortmannin, an inhibitor of intracellular IP3 kinase, an important partner in the control of actin polymerization [26]. Wortmannin (1 μM) was added to the cells' cultures for 15 min before they were exposed to three types of cargo: Tat-FAM (2.5 μM), dextran-FITC (5 μM) or albumin-FITC (5 μM, a general probe for receptor mediated endocytosis [27]) for an additional 30 min at 37 °C. Fig. 5A shows that the presence of Wortmannin has significantly hindered the uptake of albumin, dextran or Tat ($P < 0.05$, by t-test). In addition, we provide representative fluorescent microscopic images of the structural effect of wortmannin on actin's cytoskeletal network, as can be seen when comparing untreated cells (Fig. 5B) with cells exposed to wortmannin (Fig. 5C).

3.5. Dependence of uptake on plasma membrane's fluidity and electric dipole

Alteration of the plasma membrane fluidity or its electrostatic dipole potential was facilitated by incorporating cholesterol, 6KC or phloretin into the cell membrane. Membrane fluidity is a physical state defined as the freedom of molecules' movements and refers to the orientation and dynamic properties of the phospholipids' hydrocarbon chains in bilayer membranes, reflected by their anisotropy [28]. COS-7 cells were incubated at 37 °C in the presence of 0.1 mM cholesterol or 0.1 mM

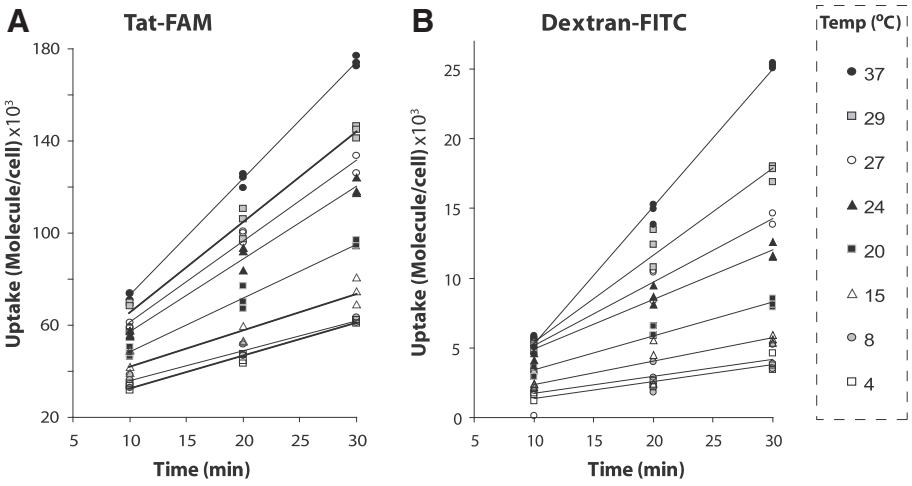

Fig. 3. Uptake kinetics at different temperatures. COS-7 cells were incubated with dextran-FITC (5 μM) or Tat-FAM (2.5 μM) at temperatures in the range of 4–37 °C for durations of 10, 20 or 30 min. Following wash and harvest procedures, cell analyses were conducted by flow-cytometry and cellular fluorescent intensity was calibrated using MESF microspheres. The uptake of Tat-FAM (A) and uptake of dextran-FITC (B) are presented as number of internalized molecules per cell as function of incubation time. Each data point in the figure denotes a triplicate average in one of 3 independent experiments. Least-square linear regression fitting was carried out at each temperature, where the regression line coefficients yield the appropriate rate of uptake (molecules/cell) at each temperature.

6KC (a cholesterol derivative with additional keto group that elevates the dipole potential of the membrane [29,30]) or 0.1 mM phloretin (which reduces the membrane dipole potential [31–33]), for 30 min. After being washed with PBS, the cells were incubated for 30 min with 5 μM TMA-DPH in PBS at 25 °C before their fluorescence polarization was measured. Fluorescence anisotropy of the cell membrane as function of membrane enrichment with cholesterol, 6KC or phloretin is presented in Fig. 6A. The addition of cholesterol to the cell membrane elevates cell membrane anisotropy, 6KC attenuated it, while phloretin had no significant influence.

To study the possible relations between plasma membrane fluidity or its dipole potential and uptake, the cells were pre-treated for 30 min with either cholesterol, 6KC, phloretin or in PBS alone (as control) as in the above section. Next, the cells were washed and further incubated at 25 ± 1 °C with either 5 μM albumin-FITC (probe for receptor mediated endocytosis [27]), 5 μM dextran-FITC or 2.5 μM Tat-FAM for the duration of 30 min. Finally, the cells were washed and harvested as described in the Methods section and their cellular fluorescence was determined by flow-cytometry. To ascertain that the cells' pre-treatments had no effect on their membrane passive permeability, these cells were incubated in the presence of 15 μM PI under similar conditions to the uptake experiments (30 min at 25 ± 1 °C) and PI incorporation into the cell nucleus was measured by flow-cytometry and compared to that of untreated cells. Both treated and untreated

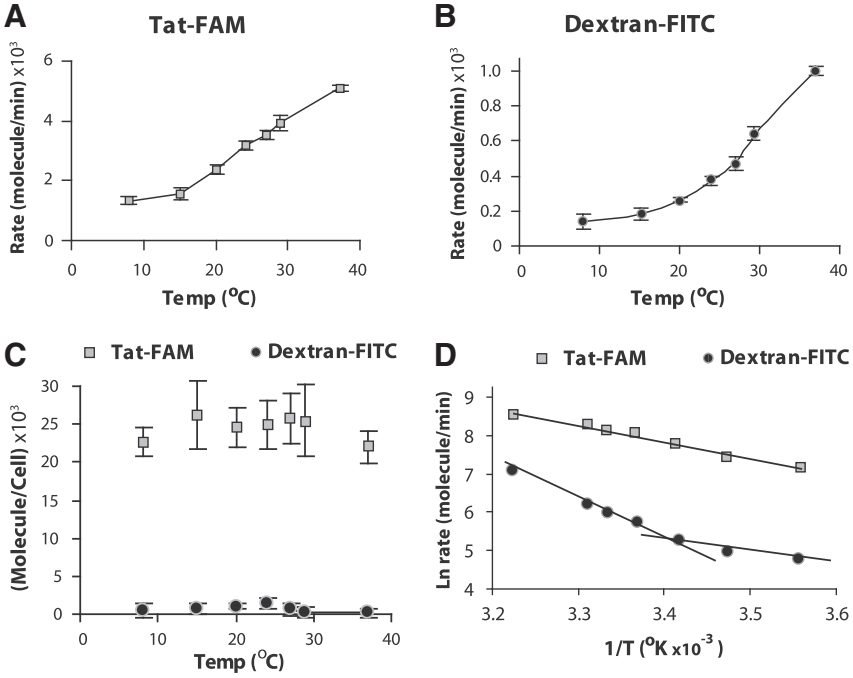

Fig. 4. The dependence of uptake rate on temperature. The rates of uptake at each temperature were calculated from data given in Fig. 3. The rates (molecules/ min) per cell of uptake as function of temperature are shown for Tat-FAM (A) and dextran-FITC (B). The values of regression lines intercept with the uptake ordinate axis (molecules/cell) in Fig. 3 are plotted as a function of temperature. The values at each temperature are given as mean ± s.d. (C). Arrhenius plots of the rates of uptake of Tat-peptide and dextran are shown in (D).

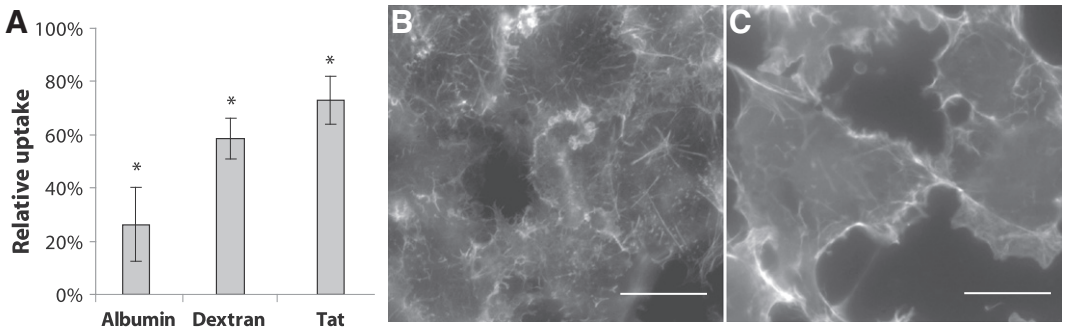

Fig. 5. The effect of the actin inhibitor Wortmannin on the uptake of dextran, albumin and Tat-peptide. COS-7 cells were exposed to 1 μM Wortmannin before and during the uptake of Tat-FAM (2.5 μM), dextran-FITC (5 μM) or albumin-FITC (5 μM). (A) Uptake of albumin, dextran or Tat-peptide was carried out for 30 min in the presence and absence of Wortmannin, at 37 °C. Results are given as mean ± s.d., in triplicates in each of 3 independent experiments * $P < 0.05$ relative to control. Representative microscopic fluorescence images of actin labeled with phalloidin in COS-7 adherent cells in the absence (B) or presence (C) of Wortmannin. Bar size in (B) and (C) is 10 μm.

cells had insignificant enhancement of PI fluorescence ($P = 0.3$ by a two-tail t-test, $n = 12$). The modulating effect, imposed by pre-treatment with cholesterol, 6KC and phloretin, on the uptake of albumin, dextran or Tat is presented in Fig. 6B in terms of percent change of each probe relative to uptake in control untreated cells. All statistical significance was tested by two tail t-test against the uptake in control untreated cells. Supplementing the cells' membrane with cholesterol elevated the uptake of albumin by 50% ($P = 0.002$) and the uptake of dextran and Tat by 25% ($P = 0.045$) each. The cells' treatment with 6KC had no significant effect on the uptake of either of the probes ($P > 0.05$). Phloretin increased the uptake of dextran by 18% ($P = 0.037$), but attenuated the uptake of Tat by 15% ($P = 0.04$), while albumin remained unaffected ($P > 0.05$).

3.6. Phloretin affects the extent of Tat uptake but not the rate of Tat endocytosis

The influence of phloretin on the rate of Tat peptide uptake was examined by first incubating the cells with 0.1 mM phloretin for 15 min, followed by addition of 2.5 μM Tat-FAM for periods of 10, 20 and 30 min at 25 ± 1 °C. Control cells were likewise incubated with Tat-FAM without pre-exposure to phloretin. The cells were washed and harvested as described in the Methods and their cellular fluorescence was analyzed by flow cytometry and calibrated using the MESF method. The data-points in Fig. 7 are fitted by the least square linear regression method and the line slopes and intercepts were calculated. The difference in the uptake rate of Tat in the presence or absence of phloretin is insignificant (3064 ± 154 and 3,185 ± 149 molecules/cell/min respectively. $P = 0.2$ by t-test). However, phloretin has attenuated the value of the regression intercept with the molecules/cell axis almost completely from 24,980 ± 3228 to 3403 ± 3338 ($P < 0.001$ by t-test).

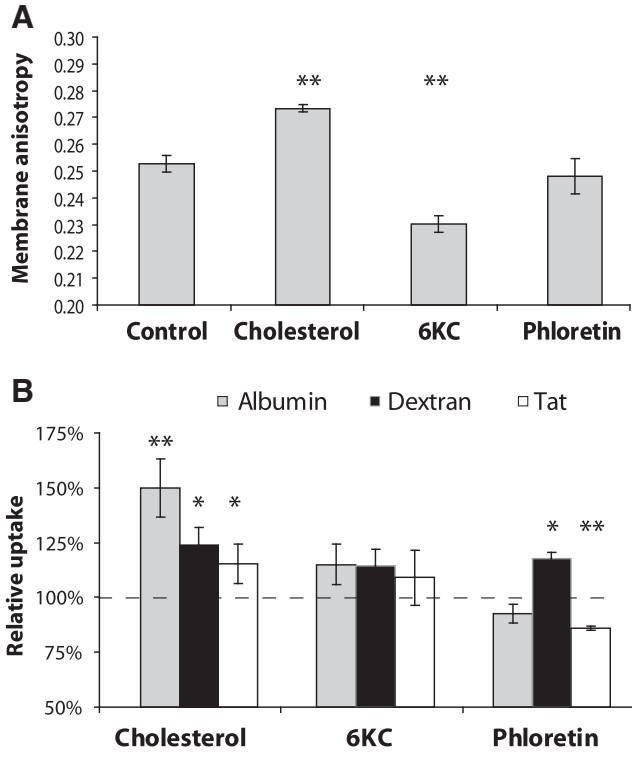

Fig. 6. Relation between TMA-DPH fluorescence anisotropy in the plasma membrane and uptake. COS-7 cells were pre-exposed to either cholesterol, 6KC, phloretin or in PBS alone for 30 min, followed by incubation with either Tat-FAM (2.5 μM), dextran-FITC (5 μM) or albumin-FITC (5 μM) for an additional 30 min. (A) Changes in cell membrane order, reflected by the rotational anisotropy of TMA-DPH in the plasma membrane, were measured by determining TMA-DPH fluorescence anisotropy following cell exposure to cholesterol, 6KC or phloretin. (B) The uptake of Tat-FAM, dextran-FITC, or albumin-FITC, was determined after wash and harvest procedures. Cell fluorescence analyses, conducted by flow-cytometry, are presented relative to control incubated in PBS, in the absence of cell membrane order modifiers. * $P < 0.05$, ** $P < 0.01$, Four replicates in each of 4 independent experiments.

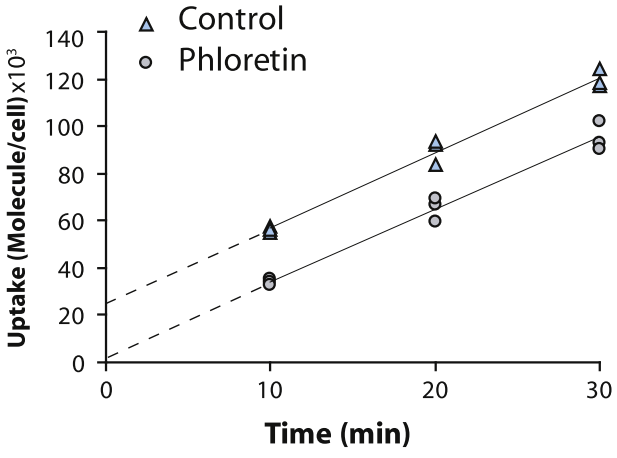

Fig. 7. The effect of phloretin on the uptake of Tat-peptide. COS-7 cells were pre-exposed to 0.1 mM phloretin or to PBS before incubation in the presence of Tat-FAM (2.5 μM) for periods of 10, 20 and 30 min. Following washing and harvesting procedures the cellular fluorescence was analyzed by flow-cytometry and calibrated using the MESF method. Least square regression ($R^2 = 0.95$) yields uptake rates of 3064 ± 154 and 3185 ± 149 (mean ± s.d.) Tat molecules/cell in the presence or absence of phloretin, respectively ($P = 0.2$). Regression line intercept with the uptake ordinate axis (illustrated by dashed line) is 3403 ± 3338 and 24,980 ± 3228 (mean ± s.d.) Tat molecules/cell, respectively ($P < 0.001$). Each data point in the figure denotes a triplicate average in 3 independent experiments.

4. Discussion

The aim of the present study is to explore the mechanisms underlying the cellular uptake of CPP, represented here by the Tat peptide. It has been convincingly shown previously that specific mutations in clathrin, dynamin or caveolin related proteins do not inhibit CPP uptake [14,15]. Therefore, we concentrated our efforts on studying the debated roles of macropinocytosis (MPC) and direct membrane translocation in the uptake of CPPs. The uptake of Tat peptide was compared with that of the polysaccharide dextran (38kD), a fluid-phase probe known to undergo uptake through MPC without participating in passive direct translocation through the cell membrane. In order to define the uptake kinetic characteristics, we selected to employ quantitative measurements of the internalized molecules and membrane order parameters, by multiple measurements at different temperatures. Quantitative analyses of uptake are achieved by measuring uptake in terms of number of molecules per cell, based on the MESF calibration method. This method allows us to quantitatively determine the uptake of dextran and of Tat, revealing that Tat enters the cells ~15 times more efficiently than dextran (Fig. 1).

We propose three possible explanations for such difference in uptake efficiency:

a) Receptor mediated vs. constitutive endocytosis: During an event of MPC, the fluid-phase is engulfed indiscriminately, thus facilitating low specificity for endocytosis. The entry of fluid-phase molecules such as dextran can thus be opportunistic, depending on non-specific MPC events. CPP, on the other hand, have been suggested to initiate MPC events by activation of membrane surface proteoglycans [34] and therefore are subjected to specific and higher rate of MPC events.
b) Difference in surface adsorption: dextran and Tat may enter the cell by sharing the same endocytic event, but due to the higher adsorption of Tat to the cell membrane, it has a higher local concentration which enables more Tat molecules to participate in any MPC event.
c) Dextran and Tat enter the cells by different uptake routes, which may share some common underlying characteristics.

To study the first possibility, we simultaneously exposed the cells to both dextran and Tat, where each probe was identified by a different fluorescence marker. If Tat is indeed inducing a higher extent of MPC events, then the entry of opportunistic fluid-phase dextran should be increased alongside. Our results, presented in Fig. 2, show that the entry of dextran is not increased in the presence of Tat, nor does Tat suffer from a competition for uptake by the presence of dextran. Therefore it is unlikely that Tat is enhancing the activation of an MPC event that could indiscriminately internalize dextran. These findings are supported by a recent report showing that the interaction of cell surface proteoglycans with CPPs has little correlation with their accumulation and uptake [35].

According to the second possible explanation, more Tat molecules can enter the cells per MPC event due to their higher local concentration at the membrane interface. Under such circumstance the same uptake event is involved in the entry of both molecules and therefore their kinetic profile should be similar. However, the study results presented for temperatures above 8 °C portray a scenario where dextran and Tat possess different uptake kinetics (Fig. 4A, B and D). The temperature dependence of Tat uptake rate between 27 and 37 °C have a Q_{10} of 1.44 and an activation energy (based on Arrhenius equation) of about 4.45 Kcal/mole. In contrast dextran uptake rate has Q_{10} of 2.17 and a biphasic Arrhenius plot possessing activation energies of E_a ~ 4.7 Kcal/mole and E_a ~ 7.2 Kcal/mole with a deflection in the region of 20–24 °C. The Q_{10} value for dextran is in line with the accepted range for an active process (i.e. between 2 and 3) such as endocytosis. The lower Q_{10} value found for Tat uptake and its lower activation energy, suggest that this process is less dependent on metabolic activity then the uptake of dextran. Furthermore, in the presence of phloretin the uptake of Tat is attenuated as opposed to the enhancing effect of phloretin on dextran uptake. Therefore, it is unlikely that the uptake of Tat and dextran shares the same mechanism of uptake. This conclusion does not necessarily mean that the two routes share no common dependencies, for example, a dependence of endocytosis on the mechanical force imposed on the membrane by actin assembly remodeling [16,36,37]. A general demonstration for such shared dependency is given by applying wortmannin, an acclaimed inhibitor of MPC which blocks the activity of intracellular IP3 kinase, an important player in the control of actin polymerization [26]. As result of the wortmannin effect on actin assembly/disassembly, the uptake of dextran (commonly attributed to fluid-phase endocytosis), Tat (assigned to CPP endocytosis) or albumin (known to be transported through receptor mediated endocytosis [27]) is all attenuated, albeit to different degrees (Fig. 4). Lowering the cells temperature can also affect actin kinetic function by lowering its assembly and rearrangement velocity through the depression of ATP hydrolysis rate [38]. The hydrolysis of ATP gradually declines with temperature and undergoes a steep decrease below 10 °C to an insignificant level at 4 °C [39]. The effect of low temperature on endocytosis is related to subduing the activity of actin and other ATP dependent force-producing proteins that are needed for driving membrane curvature and fission.

While it has been shown before that Tat peptide can undergo passive translocation across the cell membrane, it has also been claimed that active entry mechanisms are prevalent [40,41]. Our data supports the presence of an active endocytic entry mechanism of Tat into cells, by detailing the positive correlation between Tat uptake and temperature (Fig. 3). However, a detailed study of Tat uptake reveals the presence of a temperature-independent fraction (Fig. 4C), distinctive of the uptake rate. Such a low and steady component is also apparent from Fig. 3, where the uptake rate is similar between 4 and 8 °C and Tat uptake rate between 4 and 15 °C corresponds to a Q_{10} value of 1.1, complies with a passive transport. It has been previously reported that at low temperatures, a negligible rate of fluid-phase uptake exists [23–25], which may explain the low uptake of dextran, but not the relatively high presence of Tat peptide. Direct Tat adsorption to the cell external surface cannot account for the origin of the temperature-independent uptake fraction, since the presence of wash-resistant adsorbed Tat-FAM fraction has been addressed (using the TB method) and accounted for in our data.

The interplay between temperature and uptake rate can be seen in Fig. 4A and D, where a gradual transformation in uptake mechanism can explain the moderated linear plot. Supporting results are found in a previously published microscopic imaging study [6], where the intracellular distribution of CPP (oligoarginine) is shown to shift from vesicle labeling at 37 °C to diffused cytoplasmic labeling, as the incubation temperature declines 42].

In Fig. 4C, the plot intercept with the molecules/cell axis represents fast processes that introduce Tat molecules into the cell membrane and the intracellular compartment, where they are protected from the quenching effect of TB. However, the experimental study of the uptake rate by flow cytometry in the time window under 5 min represents a major experimental challenge since the process of harvesting the cells and removing the fraction of probe adsorbed to the membrane introduces a time-resolved limitation for the initial transport events. We show that the fast uptake process is independent of temperature and can be attenuated by phloretin. The origin of a fast process may come from the rapid adsorption of the peptide to the cell membrane, reported to complete in less than 5 min [43]. Such rapid adsorption is proposed by us to trigger a consequent sudden burst of uptake, before a balanced rate is instated. Similar incidence is described in a recent study of the translocation of malachite-green across bacterial cell membrane, where an initial sharp rise of the malachite-green signal indicates an initial transport rate much larger than the translocation rate through the cell membrane [44].

The attenuating effect of phloretin on Tat uptake at 25 °C (Fig. 6B) is in contrast to the effect it has on dextran endocytosis. More importantly phloretin attenuates the initial direct translocation of Tat without affecting the rate of endocytic uptake (Fig. 7), thus offering the prospect that phloretin inhibits the translocation fraction of Tat entry. A similar inhibiting effect was previously demonstrated for the amphipathic mitochondrial sequence P25 [45]. Phloretin has been previously known to decrease the permeability of hydrophobic cations [46–49]. While the mechanism by which phloretin modulates membrane permeability is yet unclear, it may be related to phloretin's ability to affect the membrane packing density by increasing the area per lipid molecule [31] as it can reduce the intra-membrane dipole potential [31–33]. Phospholipids are dipolar in character, due to the ester linkages between acidic head and the glycerol backbones, and the alignment of these dipoles creates a charge separation which gives rise to an intra-membrane dipole potential, $\Delta\psi_d$ [46], associated with packing orientation of the dipoles [50]. It should be noted that contrary to phloretin, 6KC can elevate the plasma membrane dipole potential [29,30] and yet it was found to induce only a small increment in the uptake of Tat (Fig. 6B). A possible explanation for this disparity is that phloretin can increase the area per lipid molecule in the phosphatydilcholine bilayer (from approximately 64 Å^2 to about 78 Å^2 [51]), while 6KC does not markedly change the bilayer thickness or area per lipid molecule [52].

The mechanism that underlies CPP uptake through endocytic events is unresolved as yet, but several recent studies may offer a new perspective. We would like to suggest that the positive amine residues characteristic of all CPPs, alter the electrostatic repulsion between the membrane phospholipids negative head-groups, leading to the formation of negative curvature (inward invagination) of the cell membrane and to a consequent enhanced endocytic process. The spontaneous curvature of a bilayer membrane is the equilibrium product of minimizing the elasto and electro-static forces that exist in each of its monolayers [53,54]. Reduced electrostatic repulsion force between neighboring surface charges can increase the phospholipids packing density, overcome the stabilizing surface tension force and produce membrane instability. If the surface charge density of only the external layer is decreased, the ensuing surface charge asymmetry across the bilayer can be rebalanced by the membrane adopting an inverted, negative spontaneous curvature [55–57]. For a critical value of asymmetry in surface charged density, the membrane will spontaneously bud in the absence of any applied external force [58,59]. One possible source for a decrease in membrane external surface charge density is the neutralization of the acidic phosphate head-groups by protonation. The formation of membrane spontaneous negative curvature, membrane tubulation and its internal vesiculation in response to external protonation, was demonstrated on phospholipid vesicles [60–62] and in living cells [12,13,18]. By analogy, the CPP basic amine residues may exert a similar effect, i.e. neutralizing acidic phosphate head-groups and promoting negative membrane curvature and vesicle formation. Supporting evidence for this assumption can be found in recent studies that describe CPP induced vesicle formation in model phospholipids vesicles [63–65] and red blood cells [66] which lack essential enzymes and proteins of the endocytosis machinery.

In conclusion, the present study demonstrates that the uptake process of Tat proceeds both through temperature-independent and temperature-dependent mechanisms. The temperature independent process is attributed to a direct passive translocation of Tat through the plasma membrane, whereas the temperature-dependent process is inconsistent with that of macropinocytosis and is ascribed to a yet unidentified endocytic process.

References

[1] E. Koren, V.P. Torchilin, Cell-penetrating peptides: breaking through to the other side, Trends Mol. Med. 18 (2012) 385–393.
[2] M. Lindgren, U. Langel, Classes and prediction of cell-penetrating peptides, Methods Mol. Biol. 683 (2011) 3–19.
[3] F. Madani, S. Lindberg, U. Langel, S. Futaki, A. Graslund, Mechanisms of cellular uptake of cell-penetrating peptides, J. Biophys. 2011 (2011) 414729.
[4] S. Trabulo, A.L. Cardoso, M. Mano, M.C. Pedroso de Lima, Cell-penetrating peptides: mechanisms of cellular uptake and generation of delivery systems, Pharmaceuticals 3 (2010) 961–993.
[5] A. Subrizi, E. Tuominen, A. Bunker, T. Rog, M. Antopolsky, A. Urtti, Tat(48–60) peptide amino acid sequence is not unique in its cell penetrating properties and cell-surface glycosaminoglycans inhibit its cellular uptake, J. Control. Release 158 (2012) 277–285.
[6] I.D. Alves, C.Y. Jiao, S. Aubry, B. Aussedat, F. Burlina, G. Chassaing, S. Sagan, Cell biology meets biophysics to unveil the different mechanisms of penetratin internalization in cells, Biochim. Biophys. Acta Biomembr. 1798 (2010) 2231–2239.
[7] M. Zorko, U. Langel, Cell-penetrating peptides: mechanism and kinetics of cargo delivery, Adv. Drug Deliv. Rev. 57 (2005) 529–545.
[8] A.T. Jones, E.J. Sayers, Cell entry of cell penetrating peptides: tales of tails wagging dogs, J. Control. Release 161 (2012) 582–591.
[9] G.J. Praefcke, H.T. McMahon, The dynamin superfamily: universal membrane tubulation and fission molecules? Nat. Rev. Mol. Cell Biol. 5 (2004) 133–147.
[10] S. Mayor, R.E. Pagano, Pathways of clathrin-independent endocytosis, Nat. Rev. Mol. Cell Biol. 8 (2007) 603–612.
[11] G.J. Doherty, H.T. McMahon, Mechanisms of endocytosis, Annu. Rev. Biochem. 78 (2009) 857–902.
[12] N. Ben-Dov, R. Korenstein, Enhancement of cell membrane invaginations, vesiculation and uptake of macromolecules by protonation of the cell surface, PLoS One 7 (2012) e35204.
[13] N. Ben-Dov, R. Korenstein, Actin-cytoskeleton rearrangement modulates proton-induced uptake, Exp. Cell Res. 319 (2013) 946–954.
[14] G. Ter-Avetisyan, G. Tunnemann, D. Nowak, M. Nitschke, A. Herrmann, M. Drab, M.C. Cardoso, Cell entry of arginine-rich peptides is independent of endocytosis, J. Biol. Chem. 284 (2009) 3370–3378.
[15] J.S. Wadia, R.V. Stan, S.F. Dowdy, Transducible TAT-HA fusogenic peptide enhances escape of TAT-fusion proteins after lipid raft macropinocytosis, Nat. Med. 10 (2004) 310–315.
[16] M. Al Soraj, L. He, K. Peynshaert, J. Cousaert, D. Vercauteren, K. Braeckmans, S.C. De Smedt, A.T. Jones, siRNA and pharmacological inhibition of endocytic pathways to characterize the differential role of macropinocytosis and the actin cytoskeleton on cellular uptake of dextran and cationic cell penetrating peptides octaarginine (R8) and HIV-Tat, J. Control. Release 161 (2012) 132–141.
[17] J.G. Kuhry, G. Duportail, C. Bronner, G. Laustriat, Plasma membrane fluidity measurements on whole living cells by fluorescence anisotropy of trimethylammoniumdiphenylhexatriene, Biochim. Biophys. Acta 845 (1985) 60–67.
[18] N. Ben-Dov, R. Korenstein, Proton-induced endocytosis is dependent on cell membrane fluidity, lipid-phase order and the membrane resting potential, Biochim. Biophys. Acta Biomembr. 1828 (2013) 2672–2681.
[19] V.L. Mosiman, B.K. Patterson, L. Canterero, C.L. Goolsby, Reducing cellular autofluorescence in flow cytometry: an in situ method, Cytometry 30 (1997) 151–156.
[20] S. Falcone, E. Cocucci, P. Podini, T. Kirchhausen, E. Clementi, J. Meldolesi, Macropinocytosis: regulated coordination of endocytic and exocytic membrane traffic events, J. Cell Sci. 119 (2006) 4758–4769.
[21] I.M. Kaplan, J.S. Wadia, S.F. Dowdy, Cationic TAT peptide transduction domain enters cells by macropinocytosis, J. Control. Release 102 (2005) 247–253.
[22] D.B. Peckys, F.W. Kleinhans, P. Mazur, Rectification of the water permeability in COS-7 cells at 22, 10 and 0 degrees C, PLoS One 6 (2011) e23643.
[23] Z. Mamdouh, M.C. Giocondi, R. Laprade, C. Le Grimellec, Temperature dependence of endocytosis in renal epithelial cells in culture, Biochim. Biophys. Acta 1282 (1996) 171–173.
[24] W.F. Wolkers, S.A. Looper, R.A. Fontanilla, N.M. Tsvetkova, F. Tablin, J.H. Crowe, Temperature dependence of fluid phase endocytosis coincides with membrane properties of pig platelets, Biochim. Biophys. Acta 1612 (2003) 154–163.
[25] M.K. Pratten, J.B. Lloyd, Effects of temperature, metabolic inhibitors and some other factors on fluid-phase and adsorptive pinocytosis by rat peritoneal macrophages, Biochem. J. 180 (1979) 567–571.
[26] E.H. Walker, M.E. Pacold, O. Perisic, L. Stephens, P.T. Hawkins, M.P. Wymann, R.L. Williams, Structural determinants of phosphoinositide 3-kinase inhibition by wortmannin, LY294002, quercetin, myricetin, and staurosporine, Mol. Cell 6 (2000) 909–919.
[27] R. Yumoto, H. Nishikawa, M. Okamoto, H. Katayama, J. Nagai, M. Takano, Clathrin-mediated endocytosis of FITC-albumin in alveolar type II epithelial cell line RLE-6TN, Am. J. Physiol. Lung Cell. Mol. Physiol. 290 (2006) L946–L955.
[28] L.W. Engel, F.G. Prendergast, Values for and significance of order parameters and "cone angles" of fluorophore rotation in lipid bilayers, Biochemistry 20 (1981) 7338–7345.
[29] E. Gross, R.S. Bedlack Jr., L.M. Loew, Dual-wavelength ratiometric fluorescence measurement of the membrane dipole potential, Biophys. J. 67 (1994) 208–216.
[30] M.F. Vitha, R.J. Clarke, Comparison of excitation and emission ratiometric fluorescence methods for quantifying the membrane dipole potential, Biochim. Biophys. Acta 1768 (2007) 107–114.
[31] R. Cseh, R. Benz, Interaction of phloretin with lipid monolayers: relationship between structural changes and dipole potential change, Biophys. J. 77 (1999) 1477–1488.
[32] B. Bechinger, J. Seelig, Interaction of electric dipoles with phospholipid head groups. A 2H and 31P NMR study of phloretin and phloretin analogues in phosphatidylcholine membranes, Biochemistry 30 (1991) 3923–3929.
[33] S.A. Simon, T.J. McIntosh, Magnitude of the solvation pressure depends on dipole potential, Proc. Natl. Acad. Sci. U. S. A. 86 (1989) 9263–9267.

[34] I. Nakase, A. Tadokoro, N. Kawabata, T. Takeuchi, H. Katoh, K. Hiramoto, M. Negishi, M. Nomizu, Y. Sugiura, S. Futaki, Interaction of arginine-rich peptides with membrane-associated proteoglycans is crucial for induction of actin organization and macropinocytosis, Biochemistry 46 (2007) 492–501.
[35] W.P. Verdurmen, R. Wallbrecher, S. Schmidt, J. Eilander, P. Bovee-Geurts, S. Fanghanel, J. Burck, P. Wadhwani, A.S. Ulrich, R. Brock, Cell surface clustering of heparan sulfate proteoglycans by amphipathic cell-penetrating peptides does not contribute to uptake, J. Control. Release 170 (2013) 83–91.
[36] S. Gerbal-Chaloin, C. Gondeau, G. Aldrian-Herrada, F. Heitz, C. Gauthier-Rouviere, G. Divita, First step of the cell-penetrating peptide mechanism involves Rac1 GTPase-dependent actin-network remodelling, Biol. Cell. 99 (2007) 223–238.
[37] A. Mishra, G.H. Lai, N.W. Schmidt, V.Z. Sun, A.R. Rodriguez, R. Tong, L. Tang, J. Cheng, T.J. Deming, D.T. Kamei, G.C. Wong, Translocation of HIV TAT peptide and analogues induced by multiplexed membrane and cytoskeletal interactions, Proc. Natl. Acad. Sci. U. S. A. 108 (2011) 16883–16888.
[38] M. Anson, Temperature dependence and Arrhenius activation energy of F-actin velocity generated in vitro by skeletal myosin, J. Mol. Biol. 224 (1992) 1029–1038.
[39] S. Furuike, K. Adachi, N. Sakaki, R. Shimo-Kon, H. Itoh, E. Muneyuki, M. Yoshida, K. Kinosita Jr., Temperature dependence of the rotation and hydrolysis activities of F1-ATPase, Biophys. J. 95 (2008) 761–770.
[40] I.D. Alves, C. Bechara, A. Walrant, Y. Zaltsman, C.Y. Jiao, S. Sagan, Relationships between membrane binding, affinity and cell internalization efficacy of a cell-penetrating peptide: penetratin as a case study, PLoS One 6 (2012) e24096.
[41] C.Y. Jiao, D. Delaroche, F. Burlina, I.D. Alves, G. Chassaing, S. Sagan, Translocation and endocytosis for cell-penetrating peptide internalization, J. Biol. Chem. 284 (2009) 33957–33965.
[42] M.M. Fretz, N.A. Penning, S. Al-Taei, S. Futaki, T. Takeuchi, I. Nakase, G. Storm, A.T. Jones, Temperature-, concentration- and cholesterol-dependent translocation of L- and D-octa-arginine across the plasma and nuclear membrane of CD34+ leukaemia cells, Biochem. J. 403 (2007) 335–342.
[43] G. Ruan, A. Agrawal, A.I. Marcus, S. Nie, Imaging and tracking of tat peptide-conjugated quantum dots in living cells: new insights into nanoparticle uptake, intracellular transport, and vesicle shedding, J. Am. Chem. Soc. 129 (2007) 14759–14766.
[44] J. Zeng, H.M. Eckenrode, S.M. Dounce, H.L. Dai, Time-resolved molecular transport across living cell membranes, Biophys. J. 104 (2013) 139–145.
[45] J. Cladera, P. O'Shea, Intramembrane molecular dipoles affect the membrane insertion and folding of a model amphiphilic peptide, Biophys. J. 74 (1998) 2434–2442.
[46] R.F. Flewelling, W.L. Hubbell, The membrane dipole potential in a total membrane potential model. Applications to hydrophobic ion interactions with membranes, Biophys. J. 49 (1986) 541–552.
[47] R.F. Flewelling, W.L. Hubbell, Hydrophobic ion interactions with membranes. Thermodynamic analysis of tetraphenylphosphonium binding to vesicles, Biophys. J. 49 (1986) 531–540.
[48] P.C. Jordan, Electrostatic modeling of ion pores. II. Effects attributable to the membrane dipole potential, Biophys. J. 41 (1983) 189–195.
[49] J. Schamberger, R.J. Clarke, Hydrophobic ion hydration and the magnitude of the dipole potential, Biophys. J. 82 (2002) 3081–3088.
[50] G. Le Goff, M.F. Vitha, R.J. Clarke, Orientational polarisability of lipid membrane surfaces, Biochim. Biophys. Acta 1768 (2007) 562–570.
[51] G.L. Jendrasiak, R.L. Smith, T.J. McIntosh, The effect of phloretin on the hydration of egg phosphatidylcholine multilayers, Biochim. Biophys. Acta Biomembr. 1329 (1997) 159–168.
[52] S.A. Simon, T.J. McIntosh, A.D. Magid, D. Needham, Modulation of the interbilayer hydration pressure by the addition of dipoles at the hydrocarbon/water interface, Biophys. J. 61 (1992) 786–799.
[53] M. Winterhalter, W. Helfrich, Effect of surface charge on the curvature elasticity of membranes, J. Phys. Chem. 92 (1988) 6865.
[54] M. Winterhalter, W. Helfrich, Bending elasticity of electrical charged bilayers: coupled monolayers, neutral surfaces, and balancing stresses, J. Phys. Chem. 96 (1992) 327–330.
[55] Y. Li, B.Y. Ha, Molecular theory of asymmetrically charged bilayers: preferred curvatures, Europhys. Lett. 70 (2005) 411–417.
[56] S.A. Safran, Statistical Thermodynamics of Surfaces, Interfaces, and Membranes, Addison-Wesley, 1994.
[57] M.P. Sheetz, S.J. Singer, Biological membranes as bilayer couples. A molecular mechanism of drug–erythrocyte interactions, Proc. Natl. Acad. Sci. U. S. A. 71 (1974) 4457–4461.
[58] P. Galatola, Tube formation and spontaneous budding in a fluid charged membrane, Phys. Rev. E Stat. Nonlinear Soft Matter Phys. 72 (2005) 041930.
[59] V. Kumaran, Effect of surface charges on the curvature moduli of a membrane, Phys. Rev. E Stat. Nonlinear Soft Matter Phys. 64 (2001) 051922.
[60] H. Hauser, Mechanism of spontaneous vesiculation, Proc. Natl. Acad. Sci. U. S. A. 86 (1989) 5351–5355.
[61] N. Khalifat, J.B. Fournier, M.I. Angelova, N. Puff, Lipid packing variations induced by pH in cardiolipin-containing bilayers: the driving force for the cristae-like shape instability, Biochim. Biophys. Acta 1808 (2011) 2724–2733.
[62] N. Khalifat, N. Puff, S. Bonneau, J.B. Fournier, M.I. Angelova, Membrane deformation under local pH gradient: mimicking mitochondrial cristae dynamics, Biophys. J. 95 (2008) 4924–4933.
[63] A. Lamaziere, F. Burlina, C. Wolf, G. Chassaing, G. Trugnan, J. Ayala-Sanmartin, Non-metabolic membrane tubulation and permeability induced by bioactive peptides, PLoS One 2 (2007) e201.
[64] A. Lamaziere, O. Maniti, C. Wolf, O. Lambert, G. Chassaing, G. Trugnan, J. Ayala-Sanmartin, Lipid domain separation, bilayer thickening and pearling induced by the cell penetrating peptide penetratin, Biochim. Biophys. Acta 1798 (2010) 2223–2230.
[65] A. Lamaziere, C. Wolf, O. Lambert, G. Chassaing, G. Trugnan, J. Ayala-Sanmartin, The homeodomain derived peptide Penetratin induces curvature of fluid membrane domains, PLoS One 3 (2008) e1938.
[66] H. He, J. Ye, Y. Wang, Q. Liu, H.S. Chung, Y.M. Kwon, M.C. Shin, K. Lee, V.C. Yang, Cell-penetrating peptides meditated encapsulation of protein therapeutics into intact red blood cells and its application, J. Control. Release 176 (2014) 123–132.